

7th International Building Physics Conference

# IBPC2018

---

## Proceedings

**SYRACUSE, NY, USA**

September 23 - 26, 2018

---

Healthy, Intelligent and Resilient  
Buildings and Urban Environments

[ibpc2018.org](http://ibpc2018.org) | [#ibpc2018](https://twitter.com/ibpc2018)



## **Application of Radiant Floor Heating in Large Space Buildings with Significant Cold Air Infiltration through Door Openings**

Gang Liu<sup>1</sup>, Siyu Cheng<sup>1</sup>, Yi Xu<sup>1</sup> and Kuixing Liu<sup>1</sup>

<sup>1</sup>Tianjin University, Tianjin

*\*Corresponding email: 2016206004@tju.edu.cn*

### **ABSTRACT**

Radiant Floor Heating System (RFHS) has been commonly used in railway stations in cold regions of China for its advantages in thermal comfort and energy efficiency. However, the uneven distribution and extremely cold area of the heating floor, caused by cold air infiltration through door openings, are commonly found in our field measurements. This impact is not considered in the standardized design methods, resulting in an underestimation of the design heat flux. In this paper, CFD simulations are used to quantify the impacts of natural infiltration on surface heat transfer process. Model validation was made against field measurements. 13 simulations were performed for different speeds. As a result, the mean radiant heat flux at floor surface decreased by 36.8% as the infiltration air speed increased from 0.05 m/s to 1.2 m/s, and the noneffective area increased more than 16 times. This result highlights a significant influence of natural infiltration. Regression models were finally developed as a simple method for rough estimation of this impact on radiation, which can make up the limitations of current methods and inform designers to improve their initial design of RFHS when natural infiltration is present.

### **KEYWORDS**

Radiant floor heating system (RFHS), Large space buildings, Natural infiltration, Radiation heat transfer, CFD simulations.

### **INTRODUCTION**

The proportion of radiant heat exchange in surface total heat flux counts much for the design and operation of Radiant floor heating system (hereinafter RFHS). For this system, the air temperature is allowed to be 1-2 K lower than the conventional all-air systems, due to its heat exchange mainly by radiation (Rhee K N et al, 2017). With the benefit of high energy efficiency, good thermal comfort and space saving potential, RFHS has been widely applied in most railway stations in cold regions of China and is considered as especially effective for heating this space. However, the uneven distributions and a wide low temperature region at the floor surface were commonly found in field measurements of six railway stations. This gap between the design and the reality indicates that the current design methods of RFHS are not applicable for buildings with high door opening frequency and increased ventilation heat loss. Therefore, the goals of this paper are to: 1) verify the impacts of natural infiltration on RFHS, 2) develop a simple method for rough estimation of radiation heat transfer, and 3) give reasonable advice for improving the initial design of RFHS when natural infiltration is present.

### **METHODS**

#### **Field measurement**

There are mainly 3 types of waiting hall (Fig.1), categorized by the relative position of entrance and exits. A corner type was chosen for field measurements. The test was performed from 8am to 8pm on January 8<sup>th</sup>, which was an overcast day. The measuring details are listed in Table 2. Table 1. Three types of waiting hall

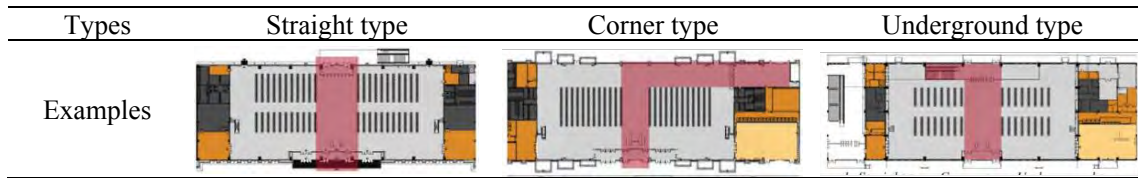





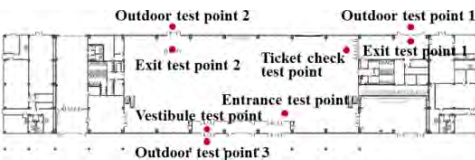


Table 2. Measuring summarization

Item	Instrument name	Range	Accuracy	Measuring points	Interval	Method
Ground temp and internal surface temp	 Sentry ST677 infrared thermometer	-32~1650°C	±2°C		2h	The average value of 5 measurements
Air temp	 HOBO UX100-003	-20~70°C	±0.21°C		5min	Air Temp and Humidity Measure Method of Public Place GB/T18204.13-2000
Airflow rate	 Tesco 425 Hot wire anemometer	0~50 m/s	±0.015 m/s		15min/h	Wind Speed Measure Method of Public Place GB/T18204.15-2000

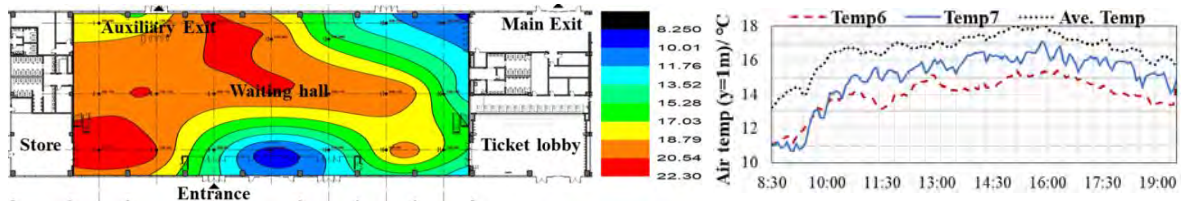


Figure 1. Measured results of waiting hall. a) Ground temp distribution, b) Air temp

The measurement interval of ground temperature was two hours. During the test period, six runs were tested, and the mean value of each point was used for interpolation. The matrix data of ground temperature was transferred into a color-filled contour image by Origin (Fig.1a). An uneven temperature distribution and a wide low-temperature region between the entrance and the main exit are observed from this image, leading to a decline of surface radiation in the combined heat transfer process. Besides, the air temperatures of point 6 and 7 are found always below average (Fig.1b), demonstrating a poor performance of convection heat transfer due to the increased ventilation heat loss.

**CFD simulation**

The ANSYS’s workbench platform was employed for CFD simulation. The size of the waiting hall is about 84 m (length)×33.6 m (width)×20.4 m (height). The geometry (Fig.2a) of the flow domain was modelled using ANSYS’s DESIGN MODELER. The developed physical model was then meshed using 3D hybrid meshing comprised of 4, 582,417 unstructured elements and 1,611,915 nodes. The maximum mesh size was 0.2 m. Meshes near wall surface are subdivided as  $y^+ < 1$  using 10 layers inflation (Fig.2b). Separate grid independency was not tested due to the fine sizes. solar radiation, internal heat gains and heat loss of enclosures were not included, since they are often counterbalanced with one another. The associated air system was shut off

during the test periods. The flow was assumed to be 3D, steady-state, incompressible and turbulent. Buoyancy was modelled with Boussinesq approximation. Near-wall treatment was considered. The heat flux generated from the heating panel was assumed as a constant value of  $80 \text{ W/m}^2$ . Based on the assumptions above, the airflow and temperature distribution were solved by the conservation laws of mass, momentum and energy. The detailed boundary conditions are given in Table 3. The airflow rates and temperatures were set equal to their actual values. Besides, RNG  $k - \epsilon$  and Discrete Ordinate (DO) model were chosen to simulate the turbulence and radiation phenomena inside the room, respectively. The coupled-analysis model was solved as steady state using SIMPLE algorithm. Enough good convergence was obtained finally.

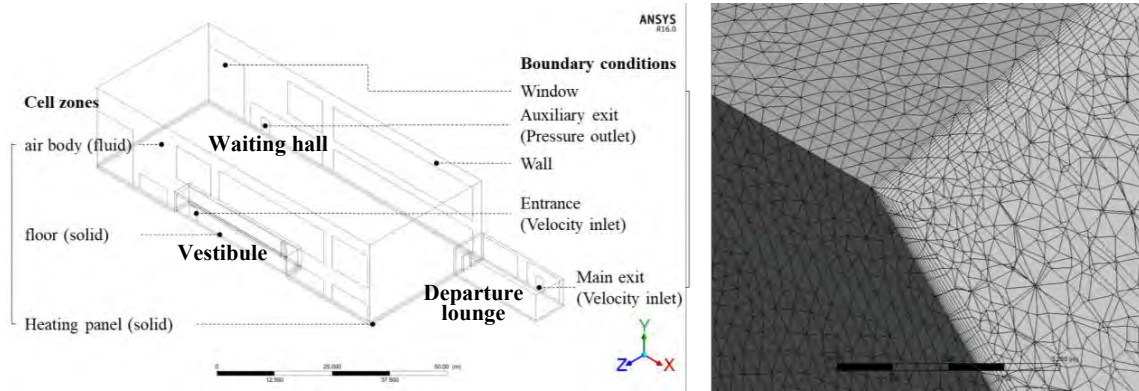


Figure 2. a) CFD drawing of the computing domain.

b) Near-wall mesh refinement

Table 3. Boundary conditions

Wall	Window	Internal wall	Floor	Heating panel
Wall temperature boundary condition ( $17^\circ\text{C}$ )	Wall temperature boundary condition ( $10.5^\circ\text{C}$ )	Adiabatic (heat flux = 0)	coupled boundary condition	Heat flux boundary condition ( $80\text{W/m}^2$ )

**Validation of the model**

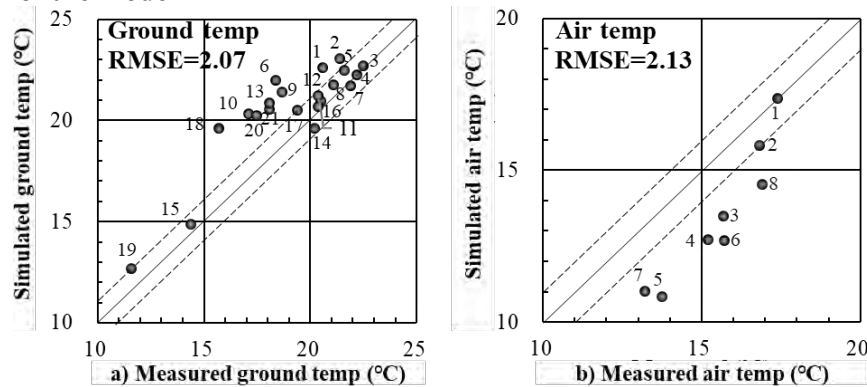


Figure 3. Correlations of actual measurements and simulated temperatures. a) Ground temperature of 21 measuring points ( $y=0$ ), b) Air temperature of 8 measuring points ( $y=1\text{m}$ ).

The measured floor surface temperatures at 21 points and air temperatures at eight points at 19:00 in the measured day were used for model validation. The occupancy rate was lowest. Fig.3 shows the correlation of actual measurement and simulation results. Dotted lines in the graphs represent the error range of  $\pm 1^\circ\text{C}$ , and RMSE denotes the root mean square error. Ground temperature shows general agreement with measurement (Fig 3a), considering the uncertainty

of 2°C with measurement accuracy of the infrared thermometer. In general, the overestimation of ground temperature may result from the assumption of constant heat flux and the limitations of steady state simulation, which neglect the temperature drop within the pipe and the delay effect of this system. This overestimation seems to be more prominent in the peripheral area, especially for points near entrance and exists (1, 6, 10, 13, 21 in Table 2). In contrast, the air temperature is much underestimated by CFD simulation (Fig 3b), especially for points in occupied area (3, 4, 5, 6 in Table 2). This discrepancy is due to the ignorance of internal load. Since the central area usually has more passengers than peripheral area, the bias error of point 1,2,7,8 was larger. Generally, these values verify the satisfactory performance of the CFD model, and the simplification allows a substantial decrease of the computational cost without affecting the performance of radiant heat exchange, which is the main interest to this study.

### Assessment parameters

The RFHS is defined as a system that radiant heat transfer covers more than 50% of heat exchange within a conditioned space. As the case mentioned in Chapter 6 of ASHRAE Handbook, HVAC Systems and Equipment (1992), the surface heat flux can be calculated separately for convection and radiation. Poor performance for providing stable thermal environment of convective heat transfer has been found in field measurements, which is caused by the increased ventilation heat loss at doors. Therefore, radiation is preferred. In this study, the overall level of radiant heat flux is viewed as an indicator of the system's thermal performance. To numerically demonstrate this, an index named mean radiant heat flux ratio (hereinafter **MRR**) is defined, which is a direct comparison of mean radiant heat flux and the total heat flux (80 W/m<sup>2</sup>) at the floor surface. Here, the mean radiant heat flux is calculated by the sum of radiant heat flux at the heating surface divided by the total heating area. Suffering from the decrease of ground temperature, the MRR may drop to 50%, which is a minimum value given in ASHRAE, or even lower. In such area the performance of the system is identified as noneffective. The ratio of the noneffective area to the total heating floor area is defined as the noneffective heating area ratio (hereinafter **NAR**). The two indices above were employed to quantify the impact of natural infiltration.

## RESULTS

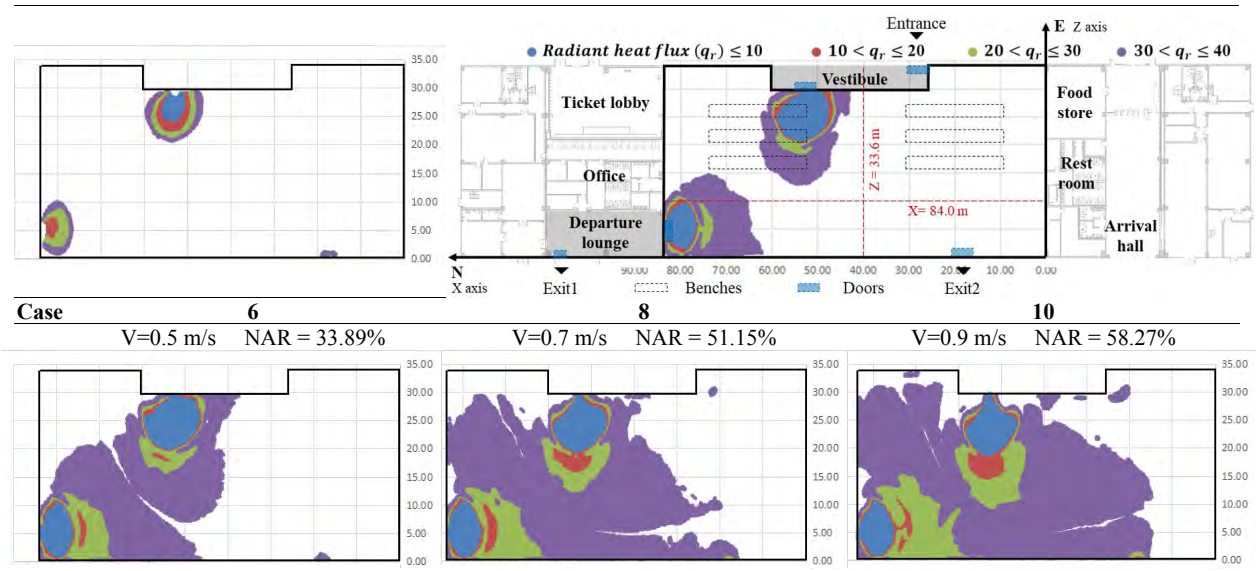
Table 4. CFD simulation results summarization

Case	1	2	3	4	5	6	7	8	9	10	11	12	13
Infiltration air speed (m/s)	0.05	0.1	0.2	0.3	0.4	0.5	0.6	0.7	0.8	0.9	1	1.1	1.2
Average radiant heat flux (W/m <sup>2</sup> )	53.0	51.4	48.2	44.3	41.33	39.0	37.2	36.0	34.9	34.1	33.3	33.6	33.5
Average convective heat flux (W/m <sup>2</sup> )	27	28.6	31.8	35.7	38.67	41	42.8	44	45.1	45.9	46.7	46.4	46.5
Mean radiant heat flux ratio (MRR)	70.0%	67.4%	61.7%	56.8%	52.9%	49.9%	47.7%	46.0%	44.6%	43.5%	42.5%	42.9%	42.8%
Noneffective heating floor area (m <sup>2</sup> )	121	150	296	494	742	956	1185	1445	1645	1775	1902	1973	2072
Noneffective area ratio (NAR)	4.3%	5.3%	10.5%	17.5%	26.3%	33.9	42.0%	51.2%	58.3%	62.9%	67.4%	69.9%	73.4%

According to the measured data, the wind speed at entrance and exits was initially set as 0.05m/s and then to increase from 0.1 to 1.2m/s at an increment of 0.1m/s. 13 scenarios in total were simulated. The main simulation results were tabulated in Table 4. Table 5 gives an intuitionistic exhibition of the noneffective heating area distributions under different wind speeds. In each figure, the noneffective area was categorized into four levels according to its radiant heat flux and filled with corresponding colors as the legend shows. The same coordinate system and room plan were only attached to case 4 as a reference. Part of cases are not shown due to limited space, but the gradually enlarging distribution pattern of the noneffective area is still obvious.

Table 5. Noneffective heating area distribution

Case	2	4
	V=0.1m/s NAR=5.34%	V=0.3 m/s NAR=17.54%



## DISCUSSIONS

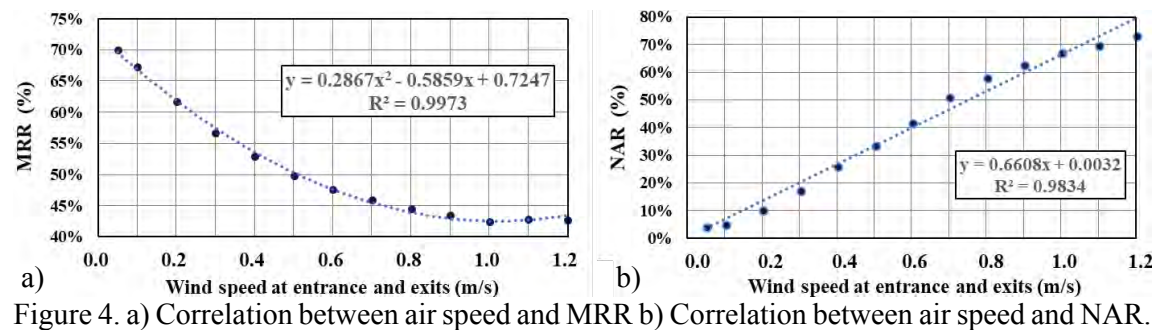


Figure 4. a) Correlation between air speed and MRR b) Correlation between air speed and NAR.

Scatterplots were used to evaluate the correlation of air velocity with MRR and NAR, and the acquired regression models were described in Fig.4.  $R^2$  values over 0.9 show significant correlations between the input and output, indicating a deep impact of wind speed on radiation heat transfer. For MRR (Fig 4a), the decreasing rate is apparently higher when the air speed is increasing from 0.05 to 0.7 m/s, implying even a slight increase of wind speed could cause a significant drop. After that, the descending rate levels off, and the lowest ratio is about 43%. For NAR (Fig 4b), it is positively related to the infiltration air speed, which is considerably low at first but grows rapidly as the wind speed increases. Taking the distribution into account, the noneffective area only appears near the entrance and exits, and the MRR of occupied area is acceptable when air velocity is low, as shown in Table 5. However, the noneffective area becomes larger and gradually spreads to the occupied area with the increase of wind speed. The occupied area thus would be at great risk of discomfort. In this way, the impact of natural infiltration could be quantified at the initial design stage once the prevailing wind speeds at the entrance and exits are given. A microscopic correlation analysis was performed between near-surface-wind-speed ( $y=1\text{mm}$ ) and the corresponding surface radiant heat flux ( $y=0$ ) to further validate the findings above by using a large sample size and taking the position factor into account. To this end, 80857 sample points were investigated and 10% of them were selected with systematic sampling method for correlation analysis. These nodes were evenly distributed at the floor surface. The result is shown in Fig 5a, taking case 6 ( $V=0.5\text{ m/s}$ ) as an example. The vertical axis represents the radiant heat flux, and the horizontal axis represents the node number which is defined sequentially according to its near-surface-wind-speed. An obvious piecewise

linear change was found at the two sides of the dividing line, which corresponds to a near-surface-wind-speed of 0.3 m/s. The left part of the dividing line shows a general decreasing trend. The discrete distribution shows a common influence of the speed and position factor. The near-surface-speed limit of 0.3 m/s and a decreasing amplitude of 33% are obtained as a design reference. While for the right part, which is replotted in Fig 5b, the highly linear correlation ( $R^2=0.85$ ) highlights the dominate influence of speed factor. The decreasing rate is apparently higher than the left, and the surface radiation is extremely low. However, this part only accounts for a small portion of the entire sample size. In all cases, the near-surface-wind-speed shows 0~1.4 m/s at the occupied area regardless of the wind speed at the entrance and exits, and the results of piecewise correlations are found to be quite similar. Therefore, case 6 is representative for all other cases.

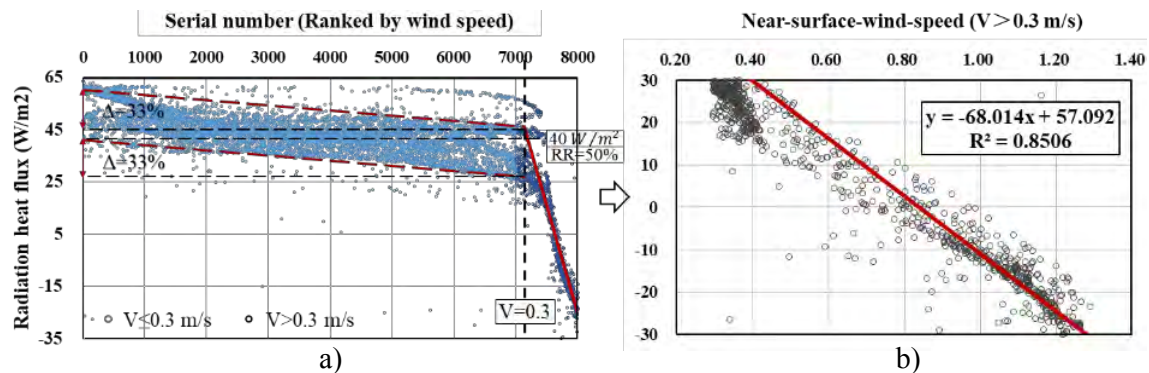


Fig.5 a) Surface radiant heat flux ( $y=0\text{mm}$ ) according to the near-surface-wind-speed ( $y=1\text{mm}$ ).  
b) the regression curve for  $V>0.3\text{m/s}$

## CONCLUSIONS

The results of field measurements provide evidences that the existing RFHS design methods are theoretically insufficient when this system operates with significant natural infiltration. Regression models for wind speed at doors and near-surface-wind-speed were developed in this paper. For a better performance of RFHS, the near-surface-wind-speed should be controlled under 0.3 m/s. Within this limit, comprehensive estimations are recommended for surface radiation, noneffective heating area and its distributions to guide reasonable design decisions. These assessments are easily to perform with the acquired regression models. When necessary, designers should take extra measures to increase the design heat flux at affected floor area, such as adding extra heat source, reducing pipe spacing or imposing the regional control methods.

## ACKNOWLEDGEMENT

The research presented in this paper was financially supported by The National Natural Science Foundation of China (the Key Program) through grant No. 51338006;

## REFERENCES

- Zhao K, Liu X H, Jiang Y. 2013. Application of radiant floor cooling in a large open space building with high-intensity solar radiation[J]. *Energy & Buildings*, 66(6):246-257.
- Rhee K N, Olesen B W, Kim K W t. 2017. Ten questions about radiant heating and cooling systems[J]. *Building & Environment*, 112367-381.
- ASHRAE. *ASHRAE handbook-HVAC systems and equipment*. 2012. Atlanta, GA: American Society of Heating, Refrigerating, and Air Conditioning Engineers.
- Yi Xu, Rui Dang, Lixiong Wang, Gang Liu. 2016. The influence study of entrance air infiltration rate on energy consumption and optimal design of the high-speed railway station in cold climate regions[J]. *PLEA 2016 32<sup>nd</sup> Conference.*, 3: 238-245